Author Manuscript

Author Manuscript

Author Manuscript

Author Manuscript

HHS Public Access

Author manuscript

Mult Scler. Author manuscript; available in PMC 2017 March 01.

Published in final edited form as:

Mult Scler. 2016 March ; 22(3): 320–328. doi:10.1177/1352458515591070.

Magnetic Resonance Imaging of the Cervical Spinal Cord in Multiple Sclerosis at 7T

Adrienne N. Dula[a,c], **Siddharama Pawate**[b], **Richard D. Dortch**[a,c], **Robert L. Barry**[a,c], **Kristen M. George-Durrett**[c], **Bailey D. Lyttle**[e], **Lindsey M. Dethrage**[c], **John C. Gore**[a,c,d], and **Seth A. Smith**[†,a,c,d]

[a]Departmet of Radiology and Radiological Sciences, Vanderbilt University Medical Center, Nashville, TN, USA

[b]Department of Neurology, Vanderbilt University Medical Center, Nashville, TN, USA

[c]Vanderbilt University Institute of Imaging Science, Vanderbilt University Medical Center, Nashville, TN, USA

[d]Department of Biomedical Engineering, Vanderbilt University Medical Center, Nashville, TN, USA

[e]Department of Neuroscience, Vanderbilt University Medical Center, Nashville, TN, USA

Abstract

Background—The clinical course of MS is mainly attributable to cervical and upper thoracic spinal cord dysfunction. High-resolution, 7T anatomical imaging of the cervical spinal cord is presented. Image contrast between gray/white matter and lesions surpasses conventional, clinical T_1- and T_2-weighted sequences at lower field strengths.

Objective—To study the spinal cord of healthy controls and patients with MS using magnetic resonance imaging at 7T.

Methods—Axial (C2-C5) T_1- and T_2*-weighted and sagittal T_2*-/spin-density-weighted images were acquired at 7T in 13 healthy volunteers (age 22-40 years), and 15 clinically diagnosed MS patients (age 19-53 years, EDSS 0-3) in addition to clinical 3T scans. In healthy volunteers, a high-resolution multi-echo gradient echo scan was obtained over the same geometry at both fields. Evaluation included signal and contrast to noise ratios and lesion counts for healthy and patient volunteers, respectively.

Results/Conclusion—High-resolution images at 7T exceeded resolutions reported at lower field strengths. Gray and white matter were sharply demarcated and MS lesions were more readily visualized at 7T compared to clinical acquisitions. with lesions apparent at both fields. Nerve roots were clearly visualized. White matter lesion counts averaged 4.7 vs. 3.1 (52% increase) per patient at 7T vs. 3T, respectively ($p = 0.05$).

[†]Corresponding Author: Seth A. Smith, Vanderbilt University Institute of Imaging Science, 1161 21st Ave South, Nashville, TN 37232, seth.smith@vanderbilt.edu, W: 615-322-6211, F: 615-322-0734.

Author Manuscript Author Manuscript Author Manuscript Author Manuscript

Keywords

MRI; Multiple Sclerosis; Spinal Cord 7T

Introduction

The spinal cord (SC) is the link between the brain and the peripheral nervous system and is involved in 90% of MS patients.[1, 2] Its somatotopic organization allows for better correlation between cord damage and neurological dysfunction.[3] Unfortunately, conventional SC MRI is insensitive to small lesions, tissues with a discontinuity between progressive damage and inflammation[4] or to non-inflammatory damage in diseases such as Adrenomyeloneuropathy[5]. Better visualization of the pathological picture may further aid in diagnosing and managing MS.[6, 7] Detecting spinal cord lesions is challenging, primarily due to their smaller size, reduced inflammation, and sub-optimal MRI methods; there is a need for MRI to address this radiological challenge.

The majority of clinical MRI uses 1.5T scanners to minimize susceptibility and transmit field inhomogeneity; however, the signal to noise ratio (SNR) and attainable resolution at 1.5T are insufficient to detect smaller lesions. Furthermore, the longer scan times necessitated by 1.5T amplify motion artifacts, and recently, 3T MRI has been considered as an alternative, but may still provide suboptimal resolution and SNR. Correlations between SC atrophy or T_2-hyperintense SC lesions and clinical disability have been modest at 3T although improved over1.5T.[8, 9] Thus, we propose that clinical MRI at lower field strengths is not able to capture the magnitude of SC involvement and often is poorly related to neurological function.[9, 10]

There are several limitations to improving SC MRI such as low SNR, demand for high resolution, and detrimental influence of physiological (cardiac, respiration, cerebrospinal fluid flow) motion. The former is improved at higher field strengths such as 7T and the increased SNR can be leveraged for higher resolution or shorter exam times. Sigmund et al.[11] demonstrated that gray/white contrast within the cervical SC is improved at 7T. It has been shown that 7T brain MRI offers greater sensitivity to gray matter (GM) lesions[12] and we hypothesize that optimized T_1- and T_2*-weighted MRI acquisitions at 7T can better visualize and quantify SC damage in MS addressing the disparity between radiological findings and neurological dysfunction.

The need for higher magnetic field strengths in assessing MS is ultimately linked to patient outcome, but in the SC, the magnitude of involvement has not been often appreciated in vivo. Here, we present our initial experience with 7T cervical SC MRI in comparison to 3T standard of care and highlight the improved visualization of lesions in MS. As with previous field strength improvements, the associations between MRI indices and clinical impairment are stronger.[13] At high field, sensitivity to Gadolinium (Gd)-enhancing lesions is improved due to increased T_1 of CNS tissue,[14] which is critical for patient safety in that decreased doses of Gd are necessary at higher fields.[15, 16] Importantly, an increase in lesion conspicuity provides a more sensitive means of monitoring therapies in exploratory trials

Author Manuscript Author Manuscript Author Manuscript Author Manuscript

and earlier detection of abnormalities, particularly in the case of reversible lesions, may aid in determining the course of therapy.

Methods

7T MRI

The local institutional review board approved all studies and informed consent was obtained prior to any scanning activity. Scans were acquired using a 7T Philips Achieva (Philips Healthcare, Cleveland, USA) scanner with a quadrature transmit and 16-channel receive spinal cord array (Nova Medical, Wilmington, MA). Shimming was performed over a volume placed within the spinal canal from C1-C7. Prior to anatomical imaging, B_1 and B_0 maps were obtained to evaluate the actual flip-angle achieved[17] and the robustness of higher-order shimming, respectively. Axial (from C2-C5) T_1- and T_2*-weighted and sagittal T_2*-/spin-density-weighted images were acquired in 13 healthy volunteers (3 female, 10 male, age = 30 ± 6, range 22-40 years), and 15 MS patients (14 relapsing-remitting, 1 primary-progressive, age 19-53, EDSS 0-3). No participant had any adverse events related to 7T scanning that required removal from the study. Sequence parameters were chosen to empirically optimize image quality and were as follows. Axial T_1-weighted – 3D fast field echo (FFE), TR/TE/α = 50ms/11ms/100°, field of view (AP × RL) = 150 × 150 mm^2, nominal resolution = 0.6 × 0.6 mm^2reconstructed to 0.3 × 0.3 mm^2, 20 slices (4-mm thickness), SENSE acceleration = 2 (phase-encode = RL), number of signal acquisitions (NSA) = 3, and total scan time = 3:03 min. A flip angle (α) of 100° was chosen since the average observed B_1 within the cord at the level of C4 was approximately 60% of the applied value. Axial T_2*-weighted – 3D FFE, TR/TE/α = 303ms/9ms/25°, field of view = 150 × 150 mm^2, nominal resolution = 0.6 × 0.6 mm^2 reconstructed to 0.3 × 0.3 mm^2, 20 slices (4-mm thickness), SENSE acceleration = 2 (phase-encode = RL), NSA = 8, and total scan time = 5:01 min. It is important to note that we chose a 3D acquisition to minimize flow voids as at lower field strengths, the multi-slice turbo spin echo (TSE) acquisition can lead to significant flow voids that in some cases obfuscate the contrast in the axial plane. Sagittal T_2*-weighted/spin-density-weighted – multi-slice FFE, TR/TE/α = 350ms/6.4ms/20°, field of view (AP × FH) = 148 × 178 mm^2, nominal resolution = 0.9 × 0.9 mm^2 reconstructed to 0.35 × 0.35 mm^2, 11 slices (3 mm thickness), SENSE acceleration = 2 (phase-encode = FH), NSA = 6, and total scan time = 3:29 min. The total scan time for tri-planar survey, SENSE reference scan, and anatomical imaging was 14:10 min. It should be pointed out, however, for 7T exams, an in-plane resolution of 0.6 mm^2 was chosen, which is challenging to obtain at lower field without significantly compromising the scan time, but is not the maximum achievable 7T resolution.

3T MRI

All 3T acquisitions in healthy volunteers were performed on a Philips Achieva (Philips Medical Systems, Best, The Netherlands) using a single channel body coil for transmission and a 16-element neurovascular coil for signal reception. We sought to compare an optimized acquisition at 3T to 7T for healthy volunteers and thus chose the multi-echo gradient echo (mFFE)[18] for 3T versus the T_2*-weighted at 7T covering the same geometry. After a tri-planar survey and SENSE reference scan, a 3D T_1 FFE was performed to match

Author Manuscript Author Manuscript Author Manuscript Author Manuscript

the scan time at 7T. The mFFE parameters were: multi-echo (3 echoes), multi-slice FFE, TR/TE_1/TE spacing/α = 700ms/7ms/9ms/28°, field of view = 150 × 150 mm^2, nominal resolution = 0.6 × 0.6 mm^2 reconstructed to 0.3 × 0.3 mm^2, 12 slices, SENSE acceleration = 2 (phase-encode = RL), and total scan time = 4:25 min.

One healthy volunteer underwent a 3T MRI exam with three 3D T_2*-weighted acquisitions: 1) at the vendor standard resolution (1.0× 1.0 mm^2), 2) at matching scan time with slightly higher resolution (0.8 × 0.8 mm^2), and 3) matching the scan time with resolution matching the 7T T_2*-weighted acquisition (0.6 × 0.6 mm^2). Finally, an mFFE scan was performed at approximately the same scan-time and resolution for comparison to the best practice 7T T_2*-weighted scan.

Nine of 15 MS patients underwent clinical standard-of-care MRI at 3T including axial T_2-weighted TSE. The remaining six MS patients underwent clinical standard-of-care MRI at 1.5T, which was not utilized for further comparison.

Because the resolution, method of acquisition and field strength were different between the clinical standard 3T and the research 7T MRI, we chose a semi-quantitative analysis. A certified neuroimager (SP) counted the number of lesions between C2-C5 on the axial 3T T_2-weighted TSE and 7T axial T_2*-weighted data. Of note, if a lesion spanned more than one slice, it was considered only one lesion. C2-C5 was chosen as the upper and lower limit because the sensitivity profile of the 7T SC array diminishes rapidly beyond these limits.

Analysis/Statistical Considerations

For the healthy volunteers, regions of interest (ROIs) were manually delineated on the mFFE in the white matter (WM) (lateral, dorsal, and ventral columns), the GM and the surrounding cerebrospinal fluid (CSF). SNR for WM, GM and CSF were calculated along with contrast to noise ratio (CNR) for WM:GM and WM:CSF. To avoid SENSE reconstruction artifacts in the noise estimate, noise was defined as the standard deviation of the CSF signal. The SNR was calculated as the average signal divided by the noise estimate in the same slice. Importantly, the WM SNR is the average of lateral, dorsal and ventral columns (left and right). The SNR for each tissue type and the CNR between WM and GM, WM and CSF were calculated in scans at 7T and 3T on healthy volunteers. Lesion counts in patient volunteers obtained from clinical scans performed at 3T were compared with scans acquired at 7T. Wilcoxon rank-sum (Mann-Whitney U) tests for paired samples were used to assess significance.

Results

High-Resolution Anatomical Imaging at 7T – Healthy Volunteers

Figure 1 presents results at 7T from three volunteers. Figure 1A shows a sagittal T_2*-weighted acquisition, axial T_2*-weighted (top row) and T1-weighted (bottom row) FFE scans at three cervical SC levels. For the T2*-weighted scans, excellent discrimination between the butterfly shaped GM and surrounding WM can be seen. The T_1-weighted images show sharp contrast between the CSF and SC. The ventral and dorsal nerve roots are apparent at the level of C4-5 (far right column). Figure 1B shows similar protocols in two

Author Manuscript Author Manuscript Author Manuscript Author Manuscript

additional healthy volunteers. Because of the high contrast between white and gray matter, variation of the GM structures is apparent. It should also be noted that in the midsagittal slice of the sagittal T_2*-weighted images (left column) the central canal can be seen along the length of the SC.

Comparison of 3T and 7T Cord MRI in Healthy Volunteers

We compared image appearance, SNR, and CNR between 3T and 7T in healthy volunteers. Figure 2 shows a single-volunteer comparison of 7T axial T_2*-weighted acquisition to 3T clinical T_2*-weighted sequence (bottom row, left), a replica of the 7T T_2*-weighted FFE scan at the same resolution and scan time (Matched Resolution), and an optimized mFFE scan at similar scan times but lower resolution (Matched Scan Time). In addition, a 3T manufacturer standard T_1-weighted FFE is compared to the 7T acquisitions resulting in similar image quality in the same scan time. Comparisons of the T_2*-weighted images show an apparent increase in contrast between GM and WM at 7T compared to 3T for all presented images.

Comparison of SNR and CNR (Table 1) indicates that the SNR is significantly higher ($p < 0.001$) at 7T compared to the mFFE at 3T. Note that the mFFE is a combination of 3 separate images (echoes) compared to a single echo at 7T. The CNR between WM:CSF for the mFFE trended to be greater ($p = 0.13$) at 3T than at 7T, which can also be observed from Figure 2 where the 7T image (top left) exhibits visually less discrimination between SC and CSF than observed at 3T (bottom left). The CNR between WM:GM indicates 7T outperforms optimized 3T mFFE acquisition ($p = 0.02$).

Visual Evaluation of 7T MRI in MS

Figure 3 shows results from three MS patients at 7T chosen to highlight lesions in different areas of the SC. Figure 3A shows a patient with a large left lateral column lesion at C4 (yellow arrows). T_1-weighted FFE image showed a hypointensity in the same region, which may indicate a T_1 black hole.[19, 20] Figure 3B shows a sagittal T_2*-weighted image with considerable signal abnormality and atrophy although dorsal column lesions can be seen at C3 (yellow arrows). Figure 3C shows axial images obtained at two levels. At the C2 level, a large dorsal and lateral column hypterintense lesion can be seen onT_2*-weighted images concomitant with a T_1-weighted hypointense lesion (yellow arrows). Interestingly this lesion seems to involve both WM and GM. At the level of C3-4, a different phenomenon is observed where several T_2* hyperintense lesions, appear in the lateral, dorsal, and ventral columns (orange arrows), but the T_1-weighted FFE appears normal. This demonstrates the widespread nature of SC lesion prevalence in MS. The lesions seen at this level on the T_1-weighted scan are less conspicuous compared to Figure 3C left panel at C2, and may indicate that these lesions are in their earliest stage and may be a viable target for treatment.

Comparison of 3T and 7T for Detection of Lesions in MS

Representative images obtained from a healthy volunteer are shown in the left column of Figure 4 for reference. The top two rows, right panel, show six of 20 axial T_2*-weighted images obtained at 7T covering C2-C4/5 compared to the bottom two rows, right panel which show T_2-weighted TSE scans at 3T. Importantly, the 7T images show signal

Author Manuscript Author Manuscript Author Manuscript Author Manuscript

hyperintensities at every level, while at 3T only a few slices show signal At 3T (bottom panels), lesion discrimination is challenging; and even when lesions are detected at 3T, is hard to localize as purely WM, or involving both WM and GM. It should also be pointed out that by using a 3D acquisition at 7T, the flow voids easily recognized at 3T (Figure 4 bottom panels) are relatively non-existent at 7T.

As a qualitative assessment, we evaluated the visual occurrence of lesions at 3T and 7T in the 9 MS patients. Clinical standard of care axial T_2-weighted TSE acquisitions at 3T resulted in 28 lesions identified, approximately 3.1 lesions per individual. At 7T on axial acquisitions, 42 lesions were detected in these same individuals using sagittal T_2* acquisitions, a 52% increase in lesion number with 4.7 lesions per patient identified.

Discussion

The majority of clinical disability in MS can be attributed to SC dysfunction (motor, sensory, bladder/bowel). Therefore, an understanding of individual patients' SC involvement is essential for clinical evaluation, diagnosis and management. Unfortunately, the SC is a difficult radiological target due to small size, constant motion, and surrounding bone-tissue interfaces and lower field MRI may not capture the extent of SC damage in disease. We evaluated the potential of SC imaging in MS at 7T and found improved lesion conspicuity and increased number of identified lesions than at 3T.

In MS, high-resolution is necessary for SC atrophy measurements. Atrophy reflects permanent neurodegeneration in MS, yet the rate of SC atrophy is 1-1.5% per year. Assuming a cross-sectional area of 69 mm^2 [21] an annual change of 0.6 - 1 mm^2 is expected, which is readily attainable at 7T and using advanced 3T methods. We studied the SC at an in-plane resolution of 0.6 × 0.6 mm^2, which, while not prohibitive for 3T, is relatively coarse for 7T. Acquisitions at 0.5 mm isotropic may be possible and with improved sequence design (cardiac triggering, gating), SC atrophy may be characterized at much higher resolution. The high GM/WM contrast, may further improve measurements of GM atrophy.

7T could improve radiological correlations with neurological disability as increased field strength provides greater sensitivity to lesions.[22, 23] Potentially correlations at lower field strengths are hampered by insensitivity to lesions as suggested in Figure 4. Further tests are needed to compare SC lesion identification in multiple scanning planes across field strengths but our data suggests a substantial improvement in lesion conspicuity at 7T.

All MS patients enrolled were relapsing-remitting and not experiencing exacerbations. We hypothesize that 7T could aid in detecting acute changes as well as chronic degeneration. The improved CNR and SNR may further augment imaging with administration of Gadolinium. Less Gadolinium may be necessitated with similar detection thresholds (CNR), and given the standard dose, smaller lesions may be observed (SNR). Thus, we suggest that 7T may also be useful in evaluating the earliest mechanisms of acute exacerbations.

It is often difficult to compare sequences across field strengths and draw absolute conclusions about each method. We compared 7T to 3T in two ways: 1) matched scan time/

Author Manuscript Author Manuscript Author Manuscript Author Manuscript

resolution for healthy volunteers, and 2) against 3T clinical standard in MS patients. In both cases, the results are slightly biased towards 7T due to the field strength dependency of relaxation rates, and a 3T examination that is sub-optimal. Further 7T comparisons to novel, improved 3T methods such as PSIR,[24] PD, T1-weighted, T2-weighted, and T2*/MT-weighted MRI[25] should be considered. Comparisons between 7T and 3T clinical standard are hampered by different imaging sequences, coverage, and scan time. Nevertheless, Ozturk et al.[25] demonstrated that T2*-weighted 3D gradient echo improved lesion contrast over conventional TSE which is further supported by our findings at 7T.

SNR theoretically increases with field strength, yet our measured increases were less than predicted (Table 1). We propose this discrepancy is caused by two factors. First, SNR was calculated as the mean cord signal divided by the SD of CSF.[26] This is a relative SNR estimate for each slice and can be used to gauge improvement across acquisitions during sequence design and optimization but is less robust than the method presented by Kellman et al.[27] Secondly, we minimized the bias for 7T by comparing SNR from an optimized 3T research protocol (mFFE). The 3T mFFE is an average of 3 distinct echoes and the SNR scales with the square root of the number of acquisitions. We observed a relative improvement of 1.38 SNR units at 7T, however, if each of 3 echoes were considered independent and scaled the SNR of the mFFE scan by $\sqrt{3}$, then the improvement in SNR at 7T would actually be 2.35, or near the theoretical 3T-7T SNR improvement expectation. While relaxation times are field dependent. T_1 and T_2 at 3T are approximately equal for WM and GM in the SC,[28] therefore, spin-density drives the contrast between tissue types. In the brain at 7T, the difference between T_1 relaxation times for WM and GM is smaller,[29] which we assume for the SC. At 7T, the lesion-white matter contrast improvement may be influenced by more than water content alone and potentially augmented by the increased susceptibility effects. It is conceivable that BBB breakdown may change the susceptibility increasing lesion conspicuity., If the T_2* of the WM is significantly lower at 7T compared to 3T, the contrast of inflammatory lesions in the tissue may be more easily appreciated at high field simply because of decreased signal in the surrounding WM tissue.

Limitations at 7T

The goal of this study was to explore the potential for 7T with a dedicated cervical SC array to detect and characterize MS lesions. Our results suggest that 7T can improve detection of SC lesions compared to 3T, but we recognize that surveying a small section of the total spinal cord is a limitation. While better lesion detection may provide improved clinical correlations,[30] there is a need to translate these methods to the thoracic/lumbar SC. Unfortunatlely, currently there is a lack of production coils to study larger sections of the SC at 7T.

It is known that with surface coil transmission the B_1 deteriorates with depth. Consequently, we obtained B_1 maps using vendor pulse calibration revealing the B_1 within the SC was approximately 50-60% the desired value. Thus for our T_1-weighted acquisition, we adjusted the excitation pulse. Future strategies for mitigation of B_1 inhomogeneity include novel pulse design and/or calibrations.

Author Manuscript Author Manuscript Author Manuscript Author Manuscript

To minimize susceptibility effects in our acquisitions, we shimmed over a prescribed volume of CSF and SC only. Of note, in some cases, a curved neck resulted in varying B_0, which could be addressed with B_1/B_0 insensitive pulses,[31, 32] or slice-wise shimming.[33]

The use of cardiac and/or respiratory gating could offer significant improvements in image quality and resolution. The 7T acquisitions presented were only empirically optimized and measurement of T_1, T_2, and T_2* for each tissue type could further guide imaging parameters for optimized contrast. Finally, implementation of FLAIR-weighted FSE scans[34] or gadolinium injection would be appropriate next steps.

Conclusions

In conclusion, we offer a preliminary report of 7T SC MRI in patients with MS. We show the contrast between lesion and WM at 7T can be greater and the widespread involvement of the SC in MS is perhaps more significant than has been appreciated using clinical, standard-of-care MRI.

Acknowledgments

Grant Support – NIH/NIBIB K01EB009120 (SAS), NIH/NIBIB K25EB013659 (RDD), KL2 TR000446 (AND), NIH/NINDS R21NS081437 (RLB, JCG), NIH/NIBIB K99EB016689 (RLB), DOD W81XWH-13-0073 (SAS), Novartis IIRP-1456 (SP)

References

1. Hittmair K, Mallek R, Prayer D, Schindler EG, Kollegger H. Spinal cord lesions in patients with multiple sclerosis: comparison of MR pulse sequences. AJNR Am J Neuroradiol. 1996; 17:1555–65. [PubMed: 8883656]
2. Kidd D, Thorpe JW, Thompson AJ, et al. Spinal cord MRI using multi-array coils and fast spin echo. II. Findings in multiple sclerosis. Neurology. 1993; 43:2632–7. [PubMed: 8255468]
3. Zackowski KM, Smith SA, Reich DS, et al. Sensorimotor dysfunction in multiple sclerosis and column-specific magnetization transfer-imaging abnormalities in the spinal cord. Brain. 2009; 132:1200–9. [PubMed: 19297508]
4. Bruck W. Inflammatory demyelination is not central to the pathogenesis of multiple sclerosis. J Neurol. 2005; 252(Suppl 5):v10–5. [PubMed: 16254696]
5. Fatemi A, Smith SA, Dubey P, et al. Magnetization transfer MRI demonstrates spinal cord abnormalities in adrenomyeloneuropathy. Neurology. 2005; 64:1739–45. [PubMed: 15911801]
6. Gilmore CP, Bo L, Owens T, Lowe J, Esiri MM, Evangelou N. Spinal cord gray matter demyelination in multiple sclerosis-a novel pattern of residual plaque morphology. Brain Pathol. 2006; 16:202–8. [PubMed: 16911477]
7. Patrucco L, Rojas JI, Cristiano E. Assessing the value of spinal cord lesions in predicting development of multiple sclerosis in patients with clinically isolated syndromes. J Neurol. 2012; 259:1317–20. [PubMed: 22179784]
8. Sicotte NL. Magnetic resonance imaging in multiple sclerosis: the role of conventional imaging. Neurol Clin. 2011; 29:343–56. [PubMed: 21439445]
9. Strasser-Fuchs S, Enzinger C, Ropele S, Wallner M, Fazekas F. Clinically benign multiple sclerosis despite large T2 lesion load: can we explain this paradox? Mult Scler. 2008; 14:205–11. [PubMed: 17986507]
10. Barkhof F. The clinico-radiological paradox in multiple sclerosis revisited. Curr Opin Neurol. 2002; 15:239–45. [PubMed: 12045719]
11. Sigmund EE, Suero GA, Hu C, et al. High-resolution human cervical spinal cord imaging at 7 T. NMR in biomedicine. 2012; 25:891–9. [PubMed: 22183956]

Author Manuscript Author Manuscript Author Manuscript Author Manuscript

12. Kilsdonk ID, de Graaf WL, Soriano AL, et al. Multicontrast MR imaging at 7T in multiple sclerosis: highest lesion detection in cortical gray matter with 3D-FLAIR. AJNR American journal of neuroradiology. 2013; 34:791–6. [PubMed: 23042930]
13. Stankiewicz JM, Glanz BI, Healy BC, et al. Brain MRI lesion load at 1.5T and 3T versus clinical status in multiple sclerosis. J Neuroimaging. 2011; 21:e50–6. [PubMed: 19888926]
14. Sicotte NL, Voskuhl RR, Bouvier S, Klutch R, Cohen MS, Mazziotta JC. Comparison of multiple sclerosis lesions at 1.5 and 3.0 Tesla. Invest Radiol. 2003; 38:423–7. [PubMed: 12821856]
15. Willinek WA, Kuhl CK. 3.0 T neuroimaging: technical considerations and clinical applications. Neuroimaging clinics of North America. 2006; 16:217–28, ix. [PubMed: 16731361]
16. Dula, AN.; Pawate, S.; Welch, EB., et al. American Society of Neuroradiology. Vancouver, B.C; 2009. Assessment of the Diversity of Cortical and Subcortical Multiple Sclerosis Pathology and Lesions Revealed by 7 T MR Imaging.
17. Yarnykh VL. Actual flip-angle imaging in the pulsed steady state: a method for rapid three-dimensional mapping of the transmitted radiofrequency field. Magn Reson Med. 2007; 57:192–200. [PubMed: 17191242]
18. Held P, Dorenbeck U, Seitz J, Frund R, Albrich H. MRI of the abnormal cervical spinal cord using 2D spoiled gradient echo multiecho sequence (MEDIC) with magnetization transfer saturation pulse. A T2* weighted feasibility study. Journal of neuroradiology Journal de neuroradiologie. 2003; 30:83–90. [PubMed: 12717293]
19. Uhlenbrock D, Sehlen S. The value of T1-weighted images in the differentiation between MS, white matter lesions, and subcortical arteriosclerotic encephalopathy (SAE). Neuroradiology. 1989; 31:203–12. [PubMed: 2674767]
20. van Walderveen MA, Kamphorst W, Scheltens P, et al. Histopathologic correlate of hypointense lesions on T1-weighted spin-echo MRI in multiple sclerosis. Neurology. 1998; 50:1282–8. [PubMed: 9595975]
21. Kearney H, Rocca MA, Valsasina P, et al. Magnetic resonance imaging correlates of physical disability in relapse onset multiple sclerosis of long disease duration. Mult Scler. 2013; 20:72–80. [PubMed: 23812283]
22. Livshits I, Hussein S, Kennedy C, Weinstock-Guttman B, Hojnacki D, Zivadinov R. Comparison of a 1.5T standard vs. 3T optimized protocols in multiple sclerosis patients. Minerva Med. 2012; 103:97–102. [PubMed: 22513514]
23. Tallantyre EC, Morgan PS, Dixon JE, et al. A comparison of 3T and 7T in the detection of small parenchymal veins within MS lesions. Invest Radiol. 2009; 44:491–4. [PubMed: 19652606]
24. Nelson F, Poonawalla AH, Hou P, Huang F, Wolinsky JS, Narayana PA. Improved identification of intracortical lesions in multiple sclerosis with phase-sensitive inversion recovery in combination with fast double inversion recovery MR imaging. AJNR Am J Neuroradiol. 2007; 28:1645–9. [PubMed: 17885241]
25. Ozturk A, Aygun N, Smith SA, Caffo B, Calabresi PA, Reich DS. Axial 3D gradient-echo imaging for improved multiple sclerosis lesion detection in the cervical spinal cord at 3T. Neuroradiology. 2013; 55:431–9. [PubMed: 23208410]
26. Smith SA, Golay X, Fatemi A, et al. Magnetization transfer weighted imaging in the upper cervical spinal cord using cerebrospinal fluid as intersubject normalization reference (MTCSF imaging). Magn Reson Med. 2005; 54:201–6. [PubMed: 15968676]
27. Kellman P, McVeigh ER. Image reconstruction in SNR units: a general method for SNR measurement. Magn Reson Med. 2005; 54:1439–47. [PubMed: 16261576]
28. Smith SA, Edden RA, Farrell JA, Barker PB, Van Zijl PC. Measurement of T1 and T2 in the cervical spinal cord at 3 tesla. Magn Reson Med. 2008; 60:213–9. [PubMed: 18581383]
29. Rooney WD, Johnson G, Li X, et al. Magnetic field and tissue dependencies of human brain longitudinal 1H2O relaxation in vivo. Magn Reson Med. 2007; 57:308–18. [PubMed: 17260370]
30. Nair G, Absinta M, Reich DS. Optimized T1-MPRAGE sequence for better visualization of spinal cord multiple sclerosis lesions at 3T. AJNR Am J Neuroradiol. 2013; 34:2215–22. [PubMed: 23764721]
31. Moore J, Jankiewicz M, Anderson AW, Gore JC. Slice-selective excitation with B(1)(+)-insensitive composite pulses. J Magn Reson. 2012; 214:200–11. [PubMed: 22177383]

Author Manuscript Author Manuscript Author Manuscript Author Manuscript

32. Moore J, Jankiewicz M, Anderson AW, Gore JC. Evaluation of non-selective refocusing pulses for 7 T MRI. J Magn Reson. 2012; 214:212–20. [PubMed: 22177384]

33. Sengupta S, Welch EB, Zhao Y, et al. Dynamic B0 shimming at 7 T. Magn Reson Imaging. 2011; 29:483–96. [PubMed: 21398062]

34. Visser F, Zwanenburg JJ, Hoogduin JM, Luijten PR. High-resolution magnetization-prepared 3D-FLAIR imaging at 7.0 Tesla. Magn Reson Med. 2010; 64:194–202. [PubMed: 20572143]

Author Manuscript Author Manuscript Author Manuscript Author Manuscript

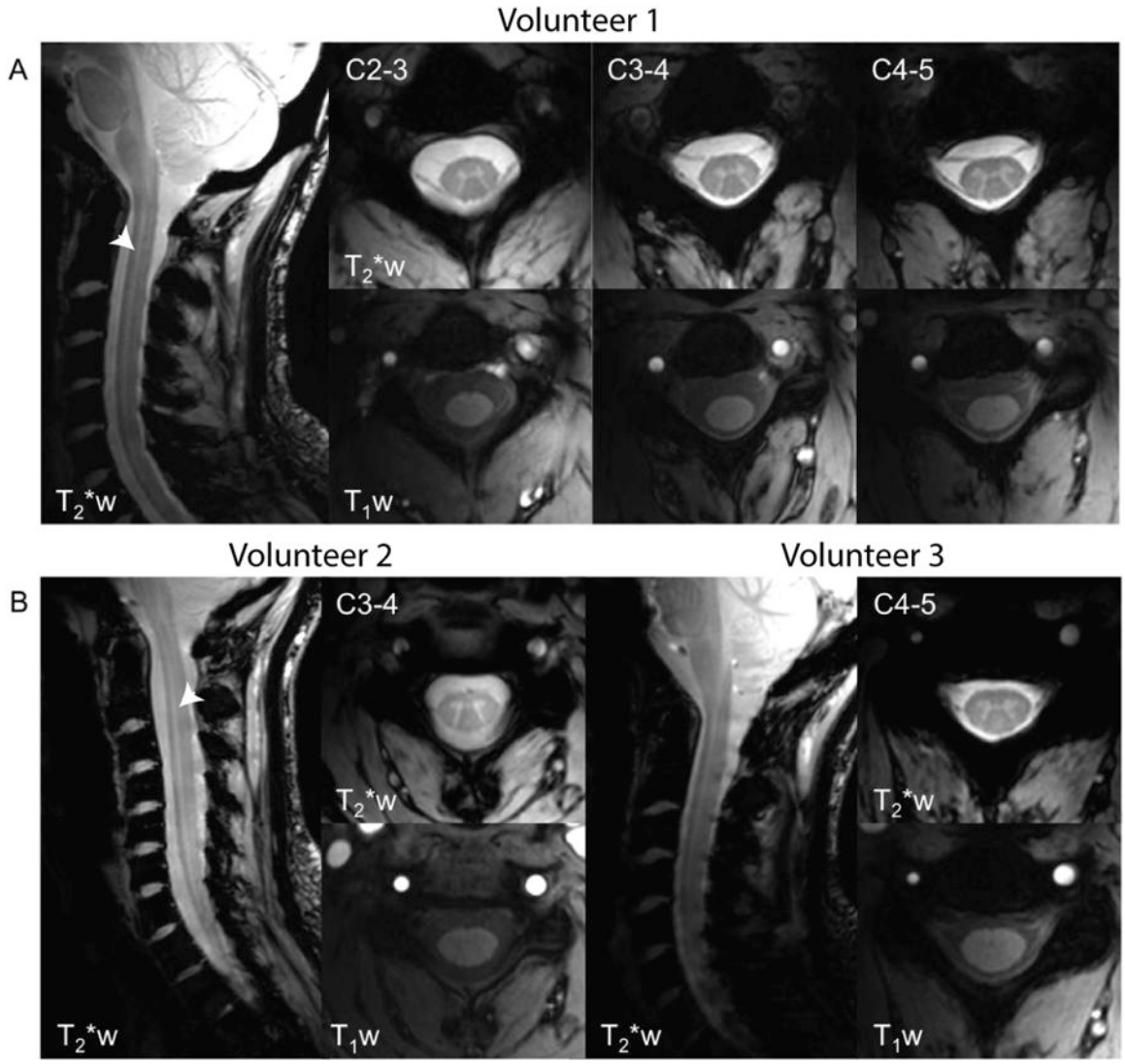

Figure 1.

Author Manuscript Author Manuscript Author Manuscript Author Manuscript

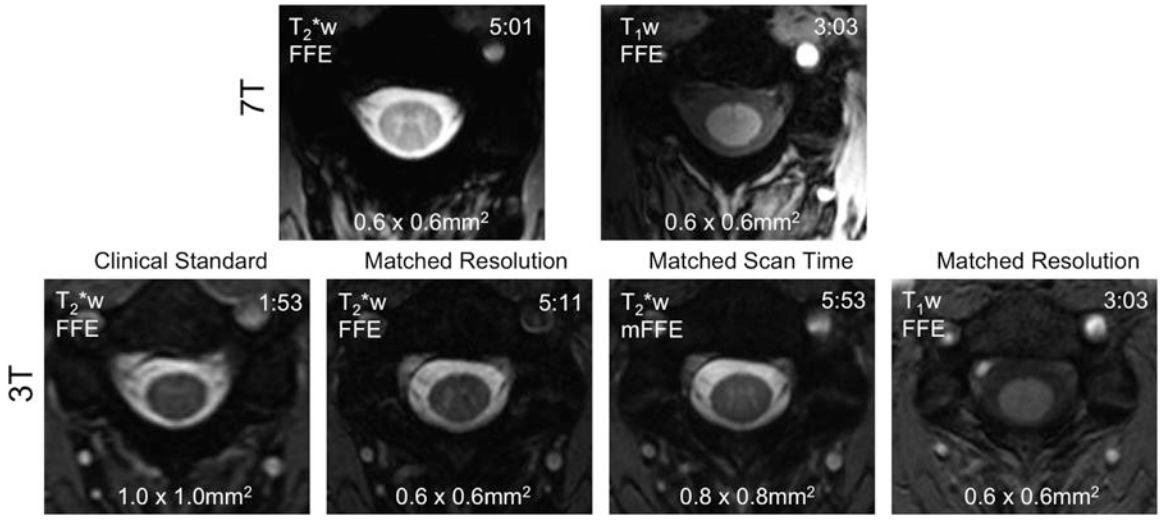

Figure 2.

Author Manuscript Author Manuscript Author Manuscript Author Manuscript

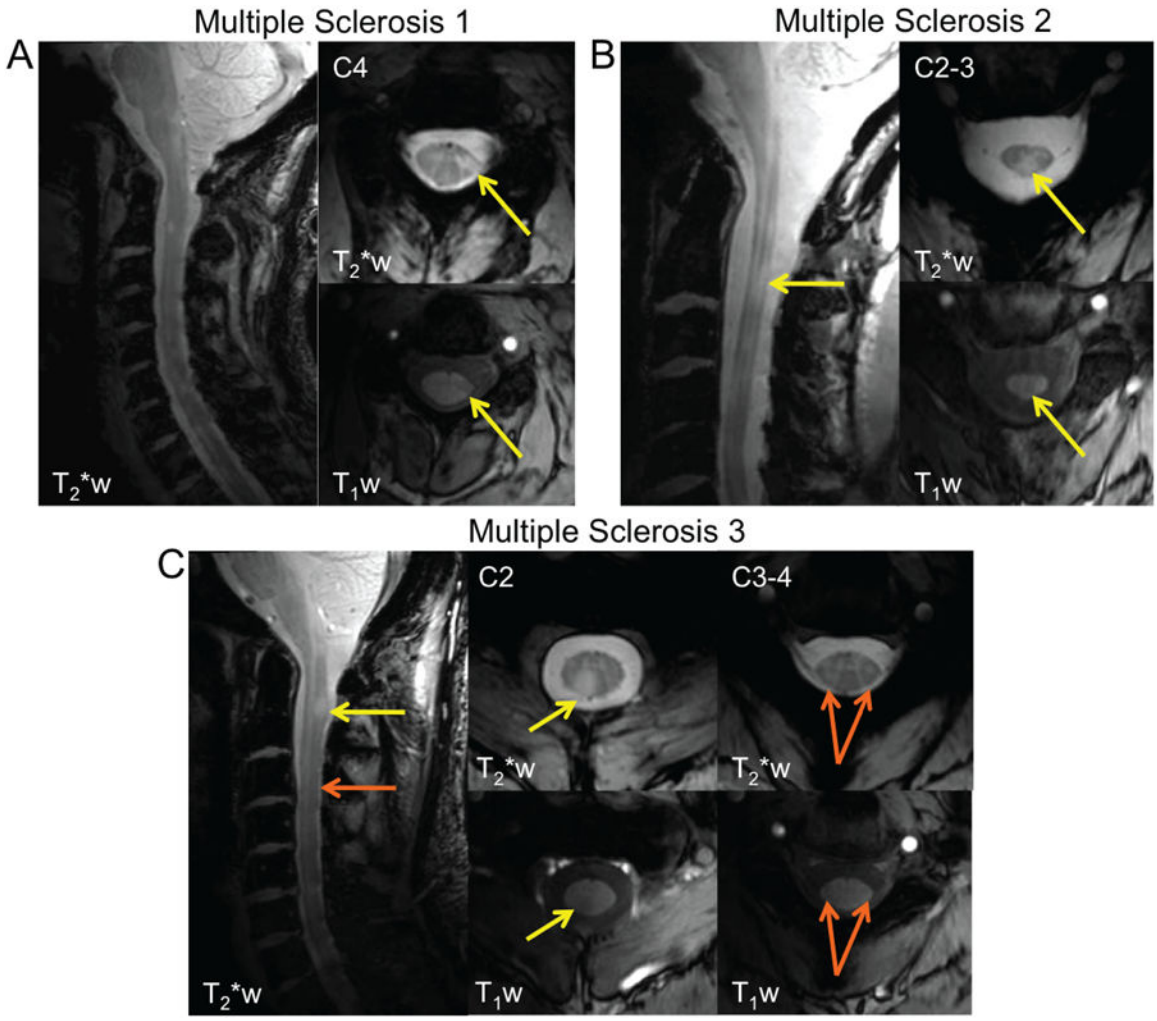

Figure 3.

Author Manuscript Author Manuscript Author Manuscript Author Manuscript

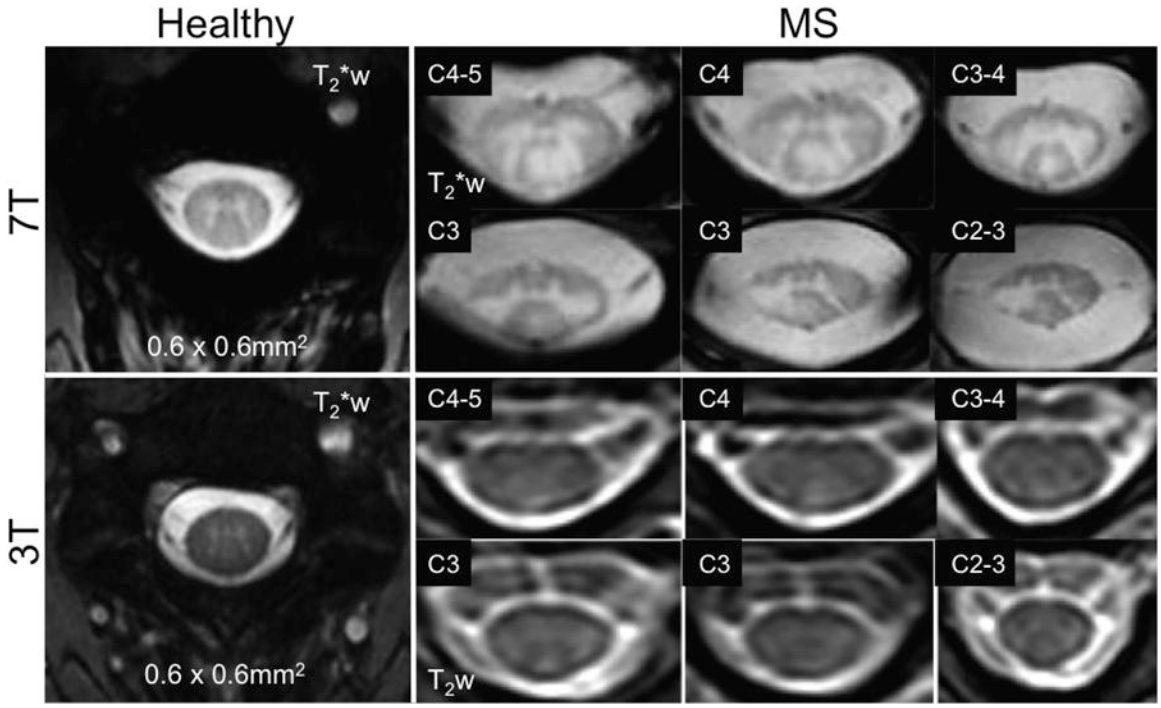

Figure 4.

Author Manuscript Author Manuscript Author Manuscript Author Manuscript

Table 1

Table 1 compares the SNR and CNR obtained at 3T and 7T and p-values are those derived from Mann-Whitney U-test for independent observations. At 7T, the SNR in WM and GM are significantly greater at 7 T compared to 3T (calculated from the optimized mFFE scans), and the CNR between WM and GM is also significantly improved at 7T. Note, however, the contrast between WM and CSF tended to be better at 3T. WM was comprised of lateral, dorsal and ventral columns.

	SNR			CNR	
	WM	**GM**	**CSF**	**WM:GM**	**WM:CSF**
3T (mFFE)	4.7 ± 1.3	5.4 ± 1.3	8.3 ± 2.4	0.63 ± 0.2	3.5 ± 1.2
7T (FFE)	6.5 ± 1.4	7.4 ± 1.7	9.4 ± 1.9	0.85 ± 0.3	2.83 ± 0.8
p-value	**$p < 0.001$**	**$p < 0.001$**	$p = 0.14$	**$p = 0.02$**	$p = 0.13$

Mult Scler. Author manuscript; available in PMC 2017 March 01.